

CHAPTER 59

Resonant Forcing of Harbors by Infragravity Waves

Gordon S. Harkins, A. M. ASCE and Michael J. Briggs¹ M. ASCE

Abstract

An extensive study of Barbers Point Harbor, including field wave gaging and numerical and physical modeling, was conducted to analyze the harbors response to infragravity wave energy. Infragravity waves have been defined as waves whose periods are greater than 25 sec. Field data collected over a 4-year period were used to calibrate the numerical model while eight extreme events were simulated in the physical model. Agreement between the numerical model, physical model, and the prototype data is good. The importance of spectral shape in the frequency domain also was analyzed by comparing the results from broad and narrow spectra.

Introduction

Frequency spectra of ocean waves consist of wind waves whose periods are less than 25 sec and longer period infragravity waves whose periods are greater than 25 sec. Although infragravity waves are rarely seen by the casual beach goer, they are important for coastal processes, including harbor seiching. Harbors with sides on the order of 500 m in length and depths on the order of 10 m are subject to harbor oscillation on the order of 1 minute and longer. Barbers Point Harbor on the Island of Oahu, Hawaii, is a prime example of a harbor that is subject to infragravity harbor resonance.

Sea and swell wave periods contribute the majority of energy in the frequency spectra. Sea waves are locally generated wind waves whose peak period is usually less than 10 sec. Sea waves also are characterized by a broad

¹ Research Hydraulic Engineer, USAE Waterways Experiment Station, Coastal Engineering Research Center, 3909 Halls Ferry Rd., Vicksburg, MS 39180.

spectrum both in direction and frequency. Swell waves, on the other hand, are generated far from the area of interest and have peak periods usually greater than 10 sec. These waves, unlike sea waves, tend to exhibit wave groupiness and have both narrow directional and frequency spectra.

Infragravity waves contribute the remaining energy in the frequency spectrum. Infragravity energy can be divided into bound and free wave energy. Bound or forced infragravity waves are nonlinearly coupled to wave groups, traveling at the group velocity of wind waves, and phase locked to sea and swell waves (Longuet-Higgins 1962). Free infragravity waves are further subdivided into leaky and edge waves.

The importance of frequency spread in the generation of infragravity energy has been widely reported from field data and theoretical analysis. Sands (1982) showed theoretically that when peakedness of the frequency spectrum increased, so did the amplitude of long-period waves generated.

This study is unique in that field wave gaging occurred prior to physical and numerical model studies. Numerical and physical models of Barbers Point Harbor were constructed to evaluate the resonant response of six different harbor expansion configurations; however, only results for the existing harbor layout will be discussed in this paper. Eight field wave cases were simulated in the physical model and compared to numerical and prototype results. To evaluate the importance of frequency spread on the generation of long-period waves, 18 empirical seas were analyzed in which the width of the frequency spectra was varied.

Description of Harbor

Barbers Point Harbor is located on the southwest coastline of Oahu, Hawaii (Figure 1). The harbor complex presently consists of an entrance channel, deep-draft harbor, barge basin, and a resort marina (often referred to as West Beach Marina). The parallel entrance channel is 140 m wide, 945 m long, and 13 m deep (MLLW). The deep-draft harbor basin is 11.6 m deep, 670 m wide, and 610 m long, covering an area of 0.37 sq km. Rubble-mound wave absorbers line approximately 1,400 linear meters of the inner shoreline of the harbor basin. The barge basin, located just seaward of the harbor on the south side of the entrance channel, is poorly sheltered from incident wave energy. It is 67 m by 400 m and is 7 m deep. The private West Beach Marina was built to the west of the deep-draft harbor. It shares the same entrance channel, is 4.6 m deep, and covers approximately 0.08 sq km. The marina was designed to accommodate 350 to 500 pleasure boats.

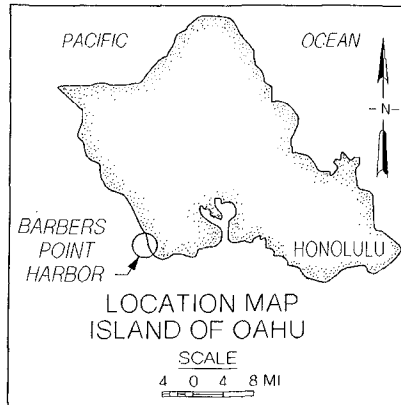


Figure 1. Project location

Prototype Measurements of Waves

Prototype measurements of waves were made in Barbers Point Harbor between July 1986 and March 1990 as part of the Monitoring Completed Coastal Projects (MCCP) Program and the Coastal Data Information Program (CDIP). These programs provide a network of real-time wave gages and are jointly sponsored by the Corps of Engineers, California Department of Boating and Waterways, and Scripps Institution of Oceanography (SIO). Figure 2 shows selected sites in the main harbor, entrance channel, and nearshore region. Bottom-mounted pressure gages were used to minimize interference with navigation (Briggs et al. 1994).

A four-gage S_{xy} array was used offshore to measure incident directional spectra conditions in 8.4 m of water. Individual gages were used elsewhere to measure frequency spectra. Other gages included the offshore (Of) and onshore (On) gages, both located shoreward of the S_{xy} gage. Channel entrance (Ce) and channel mid-point (Cm) gages were located in the entrance channel, where navigation conditions were a consideration. Finally, a gage was located in the south (Sc) corner of the harbor to measure anticipated maximum amplification factors.

A sampling scheme that collected both wind waves (energy) and long period waves (surge) was designed. Initially, energy and surge were obtained from separate records collected by each sensor: 1,024 samples at 1.0 Hz for the energy, and 2,048 samples at 0.125 Hz for the surge. After January 1989, a system upgrade permitted a single record of 4.6 hr at 0.5 Hz (8,192 samples) inside the

harbor, or 1.0 Hz (16,384 samples) outside the harbor, to be collected by each sensor.

Sampling interval was controlled by varying the call-up schedule in the software. The standard interval was every 6 hr in summer and every 3 hr in winter. A threshold routine was built into the system that automatically switched the interval back to 3 hr if significant wave height exceeded 1 m offshore, or 30 cm in the harbor. On the 3 hr schedule, an enhanced sampling scheme provided a continuous record.

The S_{xy} , C_e , C_m , and S_c gages were installed in July 1986. The S_{xy} gage experienced two major data gaps from cable failures when vessels pulling barges snagged the cable with their tow bridles. This problem was eliminated by moving the shore station to the navigation aid and re-routing the cable away from the entrance channel. Data from the second position of the S_{xy} (S_{xy2} in Figure 2) were believed to be more reliable because this gage was further from the edges of the

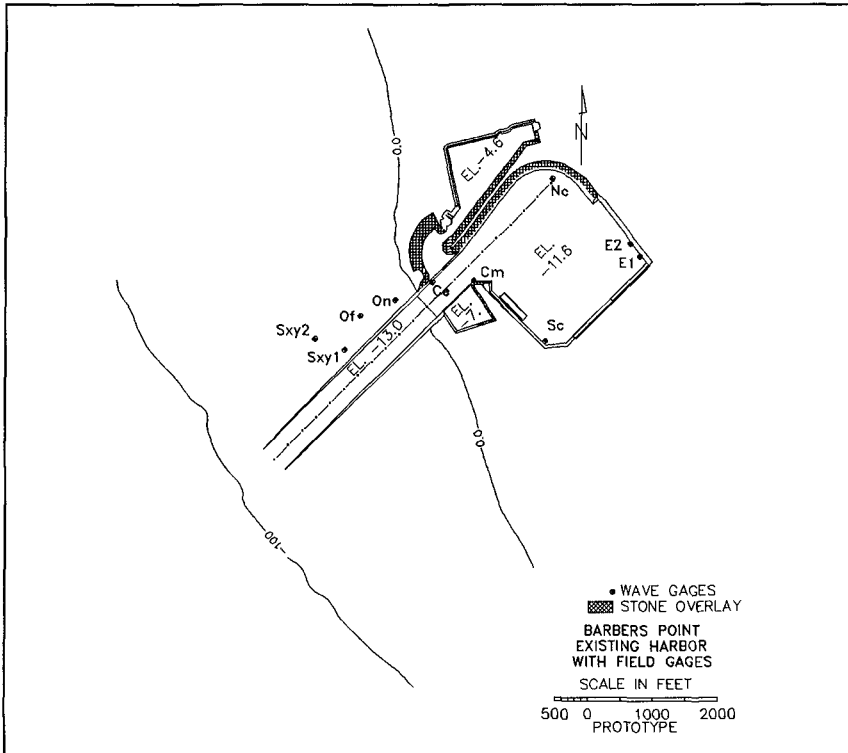


Figure 2. Prototype gage locations

entrance channel and any refractive effects which might have influenced the first position of the array. Construction in the harbor caused longer gaps in the Sc gage. In January 1989, additional sensors were installed in the north (Nc) and east corners to improve spatial resolution. The east corner gages are labeled E_1 and E_2 to differentiate the two different locations. At this time, the entire system was upgraded to the longer sampling scheme.

Numerical Model Description

The numerical harbor wave-response model, HARBD, was used to estimate wave oscillations in Barbers Point Harbor. HARBD is a steady-state finite element model which calculates linear wave oscillations in harbors of arbitrary configuration and variable bathymetry. The effects of bottom friction and boundary absorption (reflection) are included. Bottom friction is assumed to be proportional to flow velocity with a phase difference. Boundary reflection is based on a formulation similar to the impedance condition in acoustics and is expressed in terms of the wave number (i.e wavelength) and reflection coefficient of the boundary. The model uses a hybrid element solution method which involves the combination of analytical and finite element numerical solutions to determine the response of a harbor to an arbitrary forcing function.

Numerical Model Formulation

In model formulation for arbitrary depth water waves (i.e., shallow, intermediate, and deepwater waves), the water domain is divided into near and semi-infinite far regions. The near region includes the harbor and all marine structures and bathymetry of interest and is bounded by an artificial 180 deg semicircular boundary offshore of the harbor entrance. The far region is an infinite semicircular ring shape bounded by the 180 deg semicircular boundary of the near region and the coastline. The semi-infinite far region extends to infinity in all directions and is assumed to have a constant water depth and no bottom friction (Chen and Houston 1987). The finite near region, which contains the area of interest, is subdivided into a mesh of nonoverlapping triangular shaped elements. The length of side of each element is determined from the desired grid resolution and design wave parameters. The water depth and bottom friction coefficient are specified at the centroid of each element, and a reflection coefficient is assigned to each element along the solid, near region boundaries. The model requires wave period and direction as input. The solution consists of an amplification factor (i.e., the ratio of local wave height to incident wave height) and a corresponding phase angle for each grid point in the near region. Phase angle represents the difference in phase between the grid point and the incident wave. Contour plots of the amplification factors and corresponding phase angles are used to determine oscillation patterns occurring throughout the harbor.

The governing partial differential equation is derived through application

of linear wave theory to the continuity and momentum equations. All dependent variables are assumed to be periodic in time with angular frequency, ω . These steps yield the generalized Helmholtz equation (Chen 1986).

The HARBD model is intended to simulate waves which can be adequately described by the governing generalized Helmholtz equation. Therefore, HARBD does not simulate nonlinear processes such as wave breaking, wave transmission and overtopping of structures, entrance losses, steep bathymetric gradients, and wave-wave and wave-current interaction. Fortunately, these limitations are not dominant for many harbors and HARBD can be applied with some degree of confidence. Since nonlinear processes naturally occur in the prototype, consideration of these effects must be taken in interpretation of results.

A hybrid element method is used to solve the boundary value problem. In this solution, a conventional finite element approximation is used in the finite near region, while an analytical solution with unknown coefficients is used to describe the semi-infinite far region. Conditions in the near and far regions must be matched along the artificial semicircular boundary. This requirement is met by HARBD routines which automatically match the solutions, using the stationarity of a functional, to a series of Hankel Functions which give the solution for the semi-infinite far region (Farrar and Chen 1987). The hybrid element numerical techniques used in the formulation are discussed in greater detail in Chen and Mei (1974).

Numerical Model Calibration

The numerical model grid was designed with a grid resolution, the length of each element, equal to approximately one-sixth of the local wavelength, based on linear wave theory using a wave period of 10 sec and the localized water depth. After the grid was generated, individual monochromatic waves with periods from 45 to 24,576 sec were run at increments of 0.00004069 Hz (1/24,576 sec) and the results were compared to the prototype data.

The HARBD numerical model has two free parameters which can be adjusted to match prototype data: bottom friction and reflection coefficients. Other nonlinear processes such as dissipation at the sidewalls and entrance are not included in this model. The boundaries for these long-period waves were felt to be nearly perfectly reflecting. The bottom friction coefficients, however, should be a function of the type of bottom material as a function of the wave period and corresponding wavelength. Therefore, the bottom friction coefficients were varied to calibrate the model predictions to the measured prototype values at each frequency peak or mode.

The HARBD model computes a standing wave for a given frequency. For a low frequency, or very long wavelength, the entire harbor responds as if it were

a reflecting wall. A standing wave against a reflecting wall has a height of twice the incident wave. Therefore, the low-frequency wave height amplitudes predicted by HARBD for input frequencies between 0.000122 (8,196 sec) and 0.001343 (745 sec) were divided by two. Only the Helmholtz mode (or pumping mode of the harbor) was affected by this criteria because the wavelength of this wave encompasses the entire domain of the harbor and outer region to the S_{xy} gage.

The model was then tested at 0.00004069 Hz frequency increments with varying bottom friction coefficients. Resulting wave height amplifications from each test were compared with prototype measurements to investigate the reduction of wave energy due to the increase of bottom friction. This procedure was repeated until an accurate match of wave height amplification between the model predictions and prototype measurements was possible.

Physical Model Design

An undistorted, three-dimensional model of Barbers Point Harbor was constructed at a model-to-prototype scale $L_r = 1:75$, in accordance with Froude scaling laws. The nearshore area extends to the 30.5 m MLLW contour and includes approximately 1,065 m on either side of the entrance channel. Total area of the model was over 1,000 m².

Waves were generated with the directional spectral wave generator (DSWG) which can produce directional seas at multiple periods. The (DSWG) is an electronically controlled, electromechanical system, designed and built by MTS Systems Corporation, Minneapolis, MN. It is 90 ft long and consists of 60 paddles, each 1.5 ft wide and 2.5 ft high. Each wave paddle is independently driven at its joint by an electric motor operating in piston mode. This configuration, along with flexible plastic plate seals between the paddles, produces a smoother, cleaner wave form (Outlaw and Briggs 1986, Harkins 1991).

Physical Model Wave Conditions

Eight field events and eighteen empirical unidirectional spectral wave climates were generated. The eight field events were chosen from prototype wave data to obtain the largest wave height and a representative range of wave periods and direction within model constraints. All eight wave conditions represent rare events because of their large wave heights.

Directional spectra were recorded at the S_{xy} gage for the eight field events chosen. A control signal file for the 60-paddle DSWG was generated by reproducing 30 frequency bins from 0.01 - 0.3 Hz (prototype units) at 2.5° directional bins. Random phase was applied to the control signal generation and thus the long-period waves were not bound to the shorter period waves at the wavemaker. An iterative process was used until a suitable control signal spectrum

was obtained (Briggs et al. 1994).

The entrance channel is aligned approximately S45°W with the principal wave direction of the eight cases distributed around this direction. Table 1 shows the wave parameters for the simulated field wave cases.

Table 1
Simulated Target Wave Conditions

No.	Peak Period sec	Significant Wave Ht ft	Average Direction deg	Spread deg
1	12.6	7.1	80	15
2	7.7	9.8	38	17
3	8.3	7.1	45	19
4	10.0	7.4	63	16
5	9.1	10.2	58	7
6	16.7	6.5	43	14
7	16.7	8.2	43	9
8	14.2	7.1	45	9

The eighteen empirical cases consisted of three prototype wave periods (7.69, 11.11, and 16.67 sec), three principal directions (perpendicular to the shoreline and 25 and 30 deg on either side of the orthogonal) and two spectral peakedness parameters ($\gamma=3.3$ a broad spectrum, and $\gamma=7.0$ a narrow spectrum).

Long-Wave Harbor Response

Okihiro (1993) postulates that both bound and free infragravity waves are the forcing function for harbor resonance at Barbers Point Harbor. Infragravity waves are long-period waves in the range of 25 to 200 sec on the Pacific coast. Infragravity wave heights are much smaller than wind-wave heights, typically only 10 percent as large. Bound infragravity waves are non-linearly forced by and coupled to wave groups. Bound long waves appear to be the controlling mechanism when swell energy outside the harbor is large (Bowers 1977, Mei and Agnon 1989, Wu and Liu 1990). For this condition, it may be possible to predict harbor resonance given the wind-wave spectrum outside the harbor. Also, they found that wind-wave energy present at swell frequencies produces more bound wave energy than the equivalent amount of energy in sea frequencies.

Recent research (Okihiro and Seymour 1992, Elgar et al. 1992, Herbers et al. 1992, Bowers 1993) indicates that free long waves, in the form of leaky or edge waves, are important and may contribute the bulk of infragravity energy in depths corresponding to the S_{xy} location. Leaky waves are generated in shallow water and reflected or radiated seaward to the open ocean. Edge waves are generated and radiated seaward like leaky waves but become trapped on the continental shelf due to reflection and refraction and propagate in the longshore direction. Bound waves may even be a source of free infragravity waves in shallow water. The discontinuity of bound infragravity waves across the harbor mouth

may nonlinearly generate free infragravity waves. These free waves would then have energy comparable to bound long waves from outside the harbor.

Outside Barbers Point Harbor, Okihiro and Seymour (1992) found a near-shore coupling between infragravity and wind-wave energy, with a larger infragravity wave height for swell conditions than for higher frequency sea waves. Inside the harbor, they found that infragravity wave heights were highly correlated with infragravity wave heights measured outside the harbor. Furthermore, infragravity wave heights increased as swell energy increased outside the harbor.

Prototype Analysis Methods

The amplification factor $A(f)$, which is a function of frequency, was used to compare the long-period wave height outside the harbor with the long-period wave energy inside the harbor. $A(f)$ is defined as

$$A(f) = \frac{G_{yy}(f)}{G_{xx}(f)} \quad (1)$$

where G_{xx} and G_{yy} are the input and output auto-spectral density functions. The S_{xy} gage value is used as the input and the harbor gages values are used as the output. Estimates of the auto-spectral density functions $\hat{G}_{xx}(f)$ and $\hat{G}_{yy}(f)$ were obtained for each data record by breaking the 4.6-hr-long time series into 2.3-hr records and ensemble averaging the two raw spectral density functions. Estimates of the amplification factor $\hat{A}(f)$ were calculated from a linear regression on $\hat{G}_{xx}(f)$ and $\hat{G}_{yy}(f)$ from all the records as shown in Figure 3 (Lillycrop et al. 1993).

Physical Model Analysis Methods

In the physical model, a slightly different analysis method called transfer function estimates was utilized. The transfer function is defined as

$$|\hat{H}(f)| = \frac{|\hat{G}_{xy}(f)|}{\hat{G}_{xx}(f)} \quad (2)$$

where $\hat{G}_{xy}(f)$ is the cross-spectral estimate between input x and output y channels and $\hat{G}_{xx}(f)$ is the auto-spectral estimate for the input x channel. The auto-spectral estimate is just the frequency spectrum for the S_{xy2} gage for each wave case. Cross-spectral estimates are similar to auto-spectral estimates except that both input S_{xy2} and output harbor gages are used in the calculation. One advantage of the cross-spectral analysis over the auto-spectral analysis is that the estimate is not as easily biased by noise in the input or output signal (Briggs 1981). For the transfer function for the south gage (S_c), the cross-spectral estimate contains information from both the S_{xy2} and S_c gage. A single line was plotted on Figure 3

by averaging the transfer function for the eight wave cases. This increased the statistical confidence of the results.

Numerical Model Analysis Methods

To analyze long period harbor response in the numerical model, individual monochromatic waves with an amplitude of one were input with direction perpendicular to the bottom contours. The increment between wave frequency was 0.000041 Hz (1/24,576 sec) for wave periods between 45 and 24,576.1 sec. Since the numerical model was tested at three times the frequency of the analyzed prototype measurements, the results were averaged over wave periods one increment above and one increment below the prototype frequencies, analogous to band averaging. This was done so that the numerical frequencies matched those of the prototype. The single line shown in Figure 3 is thus made up of numerous runs. Since the input wave has unit amplitude, the amplification factor is simply the value of the wave amplitude at a particular location.

Model Comparison

Frequency response of prototype and physical and numerical models is shown in Figure 3. As can be seen, there is good agreement between the three. Values greater than one represent harbor resonance, since there is more energy at that particular frequency inside the harbor than outside. One might note that the physical model does not replicate the longest period resonant mode. This is because limited duration experimental runs were conducted and these long-period modes were not extractable from the data record.

Since the numerical model was tuned to existing conditions of the prototype, one would expect the results to be very similar. The reason for calibrating the numerical model was to investigate alternative harbor layouts.

The prototype results inherently show the effects of both free and bound infragravity wave energy, since both components are present in nature. The physical model was run under extreme wave events and in nature bound waves would be the principal component in the infragravity spectra for these wave conditions. To avoid reflections of wind waves off the sidewalls, wave absorbers were placed along the perimeter of the model. This also dampened the leaky wave energy released at the breaker zone which then would have to reflect off the side walls before propagating into the area of interest. Infragravity energy found in the physical model was generated from nonlinear interactions of the wind wave spectra.

Waves generated in the numerical model are analogous to free leaky waves. The numerical model is linear and is not capable of modelling nonlinear

mechanisms important for the generation of infragravity wave energy.

Independent of the forcing mechanism of infragravity waves, the harbor response is a function of harbor geometry. The numerical and physical model

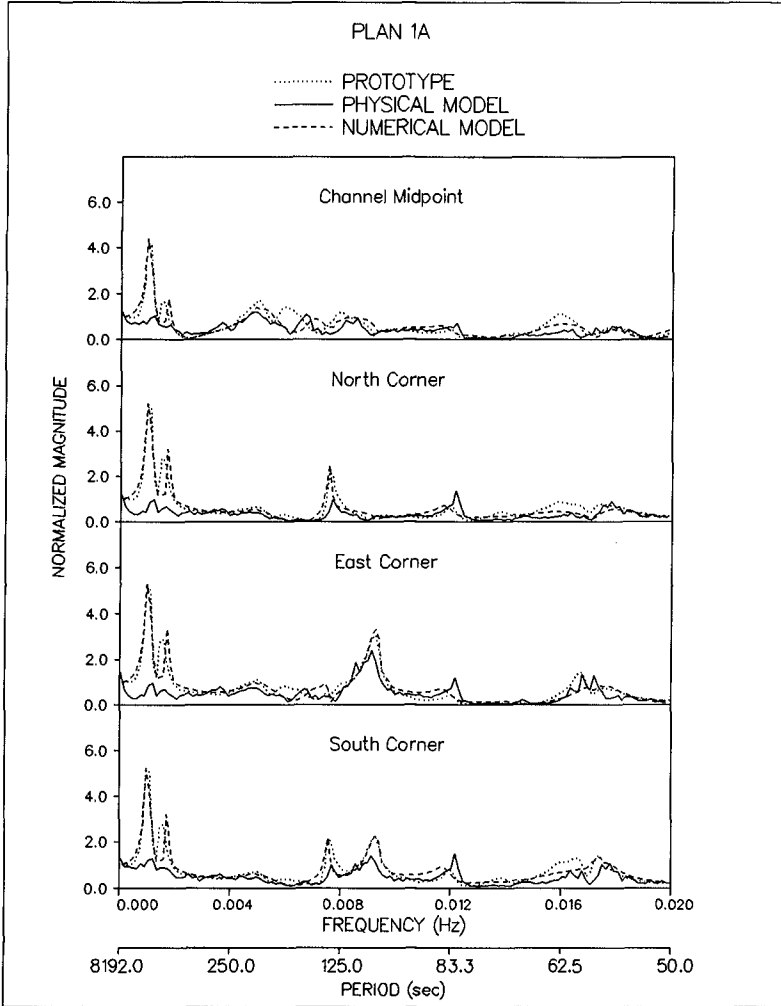


Figure 3. Transfer functions for existing harbor

accurately predict the harbor response.

Importance of Frequency Spread

The transfer functions shown in Figure 3 for the four corners show amplification or reduction of long-period waves between the S_{xy2} gage and the four corner gages. To calculate the amplitude of the long-period wave at a particular period inside the harbor, the amplitude of that wave outside the harbor must be known. In nature, there are always some low-amplitude long-period waves present, and in most cases these low levels do not interfere with ship mooring or navigation. One aspect that does appear to be important in the growth of infragravity wave energy is the peakedness of the spectra in the frequency domain.

The JONSWAP spectrum proposed by Hasselman (1973) is characterized by a parameter called the peak enhancement factor, γ , which controls the peakedness of the frequency spectra (Goda 1985). A peakedness parameter $\gamma=3.3$ (broad spectrum) was found to be the average for the results of the joint wave observation program and is characteristic of sea waves. Waves that have travelled long distances (on the order of 9,000 km) exhibited narrow banded spectrum on the order of $\gamma=8-9$ (Goda 1983).

To ascertain the importance of the peakedness parameter on generation of infragravity energy, seven gages were located along the 30-m depth contour (offshore gage array) and seven gages were located along the 8.5-m contour (nearshore gage array). The eighteen empirical wave cases then were run with two peakedness parameters. The zeroth moment m_0 or sum of the energy spectra between 25 and 660 sec was used to evaluate the growth of infragravity wave energy. By averaging results between the nine broad-band spectra for the fourteen different wave gages, there was a 183 percent increase in the infragravity wave energy between 30m and 8.5m. The nine narrow band spectra showed a growth of 224 percent between the offshore and nearshore gage arrays.

A comparison between the spectral response of two wave cases with identical parameters, except the peakedness parameter, is shown in Figure 4. The general trend shows an increase in the infragravity wave energy for the narrow band spectra.

Summary

Results from the physical and numerical models were compared against prototype data. Harbor response of the physical and numerical models showed good agreement with field data. Slightly different analysis techniques were used by each but the final results produced by each technique are comparable.

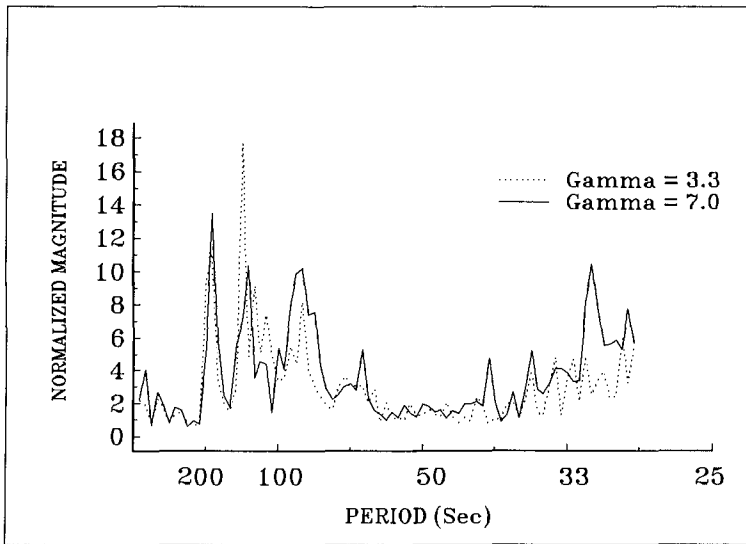


Figure 4. Comparison of infragravity growth between broad $\gamma=3.3$, and narrow $\gamma=7.0$ spectra.

Comparisons between the physical model, numerical model and field data show the resonant response of the harbor. The amplitude of long period waves in the harbor is a function of wave amplitude outside the harbor. One aspect that is important for the evolution of infragravity wave energy outside the harbor is the spectral shape of the wind wave energy in the frequency domain. The growth of infragravity wave energy was evaluated between 30m and 8.5m water depth. Empirical wave spectra with two peakedness parameters were analyzed. The physical model showed that more infragravity wave energy evolved from the narrow banded spectra then evolved from the broad banded spectra.

Acknowledgements

The authors wish to acknowledge Headquarters, U.S. Army Corps of Engineers, U.S. Army Engineer Division, Pacific Ocean (POD), and Harbors Division, Department of Transportation (HDOT), State of Hawaii for authorizing publication of this paper. It was prepared as part of a joint effort among the Civil Works Research and Development Program, Monitoring Completed Coastal Projects Program, POD, and DOT. The author would also like to thank the following individuals for their assistance and participation in this project: Messrs. Stan Boc, Dennis Markle, Edward Thompson, Ernie Smith, Frank Sargent, David Daily, Hugh Acuff, Larry Barnes and Mses. Debra R. Green and Linda Lillycrop.

Bibliography

Bowers, E.C. (1977). "Harbor Resonance Due to Set-Down Beneath Wave Groups," J. Fluid Mech., 79, pp 71-92.

Bowers, E.C. (1993). "Low Frequency Waves in Intermediate Depth," Proceedings of 23rd International Conference on Coastal Engineering (ICCE).

Briggs, M. J. (1981). "Multichannel Maximum Entropy Method of Spectral Analysis Applied to Offshore Structures," M.S. thesis, Massachusetts Institute of Technology.

Briggs, M. J., Lillycrop, L. S., Harkins, G. S., Thompson, E. F., and Green, D. R. (1994). "Physical and Numerical Model Studies of Barbers Point Harbor, Oahu, Hawaii," Technical Report CERC-94-14, U.S. Army Engineer Waterways Experiment Station, Vicksburg, MS.

Chen, H. S. (1986). "Effects of Bottom Friction and Boundary Absorption on Water Wave Scattering," Applied Ocean Research, Vol 8, No. 2, pp 99-104.

Chen, H. S. and Houston, J. R. (1987). "Calculation of Water Oscillation in Coastal Harbors: HARBS and HARBD User's Manual," Instruction Report CERC-87-2, U.S. Army Engineer Waterways Experiment Station, Vicksburg, MS.

Chen, H. S., and Mei, C. C. (1974). "Oscillations and Wave Forces in an Offshore Harbor," Report No. 190, Department of Civil Engineering, Massachusetts Institute of Technology, Cambridge, MA.

Elgar, S., Herbers, T. C., Okihiro, M., Oltman-Shay, J., and Guza, R. T., (1992). "Observations of Infragravity Waves," Journal of Geophysical Research, Vol 97, No. C10, 15573-15577.

Farrar, P. D., and Chen, H. S. (1987). "Wave Response of the Proposed Harbor at Agat, Guam: Numerical Model Investigation," Technical Report CERC-97-4, US Army Engineer Waterways Experiment Station, Vicksburg, Miss.

Goda, Y. (1985) *Random Seas and Design of Maritime Structures*. University of Tokyo Press, Toyko, Japan.

Goda, Y. "Analysis of Wave Grouping and Spectra of Long-Travelled Swell", Rept. Port and Harbour Res. Inst., Vol 299, 1983, pp. 3-41.

Harkins, G. S. (1991). "Sensitivity Analysis For Multi-Element Wavemakers," Thesis presented to the University of Delaware in partial fulfillment of the requirements of the Degree of Masters of Applied Science.

Hasselmann, K. et al. Measurement of Wind Wave-Growth and Swell Decay During the Joint North Sea Wave Project (JONSWAP), Deutsche Hydr. Zeit, Reihe A (8°), No. 12, 1973.

Herbers, T. C., Elgar, S., Guza, R. T., and O'Reilly, W. C. (1992). "Infragravity-frequency (0.005-0.05 Hz) Motions on the Shelf," Proceedings of 23rd International Conference on Coastal Engineering (ICCE).

Lillycrop, L. S., Briggs, M. J., Harkins, G. S., Boc, S. J., and Okihiro, M. S. (1993b). "Barbers Point Harbor, Oahu, Hawaii monitoring study," Technical Report CERC-93-18, U.S. Army Engineer Waterways Experiment Station, Vicksburg, MS.

Longuet-Higgins, M. S. (1962). Resonant Interaction Between Two Trains of Gravity Waves, *J. Fluid Mech.*, Vol 12, pp 321-332.

Mei, C.C., and Agnon, Y. (1989). "Long-Period Oscillations in a Harbor Induced by Incident Short Waves," *J. Fluid Mech.*, Vol 208, pp 595-608.

Okihiro, M., (1993). "Seiche in a Small Harbor," Dissertation presented to the Scripps Institution of Oceanography, University of California, San Diego, in partial fulfillment of the requirements of the Degree of Doctor of Philosophy in Oceanography.

Okihiro, M., and Seymour, R. J. (1992). "Barbers Point Harbor Resonance Study," Scripps Institute of Oceanography, (unpublished manuscript), pp 1-26.

Outlaw, D. G., and Briggs, M. J. (1986). "Directional Irregular Wave Generator Design for Shallow Wave Basins," 21st American Towing Tank Conference, August 7, Washington, D.C., pp 1-6.

Sands, S. E., (1982) Long Waves in Directional Seas, *Coastal Engineering*, 6, 195-208.

Wu, J.-K., and Liu, P.L.-F. (1990). "Harbor Excitations by Incident Wave Groups," *J. Fluid Mech.*, Vol 217, pp 595-613.